A parametric life-cycle model for assessing environmental impacts of 4G and 5G cellular base stations

Louis Golard*, louis.golard@uclouvain.be
Robin Dethienne*, robin.dethienne@uclouvain.be
Jérôme Louveaux*, jerome.louveaux@uclouvain.be
David Bol*, david.bol@uclouvain.be
*ICTEAM – UCLouvain, Louvain-la-Neuve, Belgium

Declarations

Data availability Processed presentations of the data supporting the results of this study are available in the Supplementary Information. Part of the raw data is used under license for this study and is subject to availability restrictions. Access to the licensed ecoinvent version 3.10 database is required to calculate the results of this study.

Author contributions (following the CRediT taxonomy) Louis Golard, Robin Dethienne: conceptualization, methodology, investigation, resources, software, writing. Jérôme Louveaux, David Bol: conceptualization, methodology, resources, writing, supervision.

Funding This study was supported by Proximus, by the EECONE project funded by the Chips Joint Undertaking under grant agreement 101112065, and by the Fonds européen de développement régional (FEDER) and the Wallonia within the Wallonie-2020.EU Program.

Competing interests The authors have no relevant financial or non-financial interests to disclose.

Abstract

Purpose This paper presents a parametric life-cycle model to assess the environmental impacts of multi-band 4G and 5G sub-6 GHz cellular base stations. While most existing studies emphasize operational energy consumption, our model covers all life-cycle stages with a focus on the production stage. It is designed to support the eco-design of base stations and optimize the deployment strategies of radio access networks as they rapidly evolve to support the dramatic growth in mobile data traffic.

Methods The proposed model is configurable according to variables representing features controlled by network operators and operating conditions imposed by users and follows a parametric functional unit to enhance flexibility. It is organized into parametric modules that differentiate between base station components and life-cycle stages, and comprise multiple foreground processes. The corresponding impact assessment factors are calculated from background modeling using ecoinvent 3.10 with the multi-indicator method Environmental Footprint 3.1. Approximate numerical model parameters are obtained from regression analyses based on detailed component teardowns, manufacturer technical documentation and network operator information, thereby enabling quantitative comparisons between base station configurations. Furthermore, uncertainty in the model and numerical estimates is quantified by estimating variability of regressions and by assessing modeling errors.

Results and discussion Life-cycle assessment results are obtained by applying the model to six typical base station configurations. Among all impact indicators, the results show that energy consumption in the use stage accounts for 80% to >95% of total global warming potential, and that the production stage is the second largest contributor with a range of 1000 to 4000 kg CO_2 eq per base station. Conversely, the use of mineral and metal resources is more balanced between the production and use stages. Although macro base stations have a greater impact per unit than micro base stations, they also have greater coverage and capacity, which benefits their impact per communication service provided. Moreover, uncertainty analysis shows an interquartile range of ±20% with respect to the median of stochastic assessments.

Conclusions Thanks to its flexibility, the proposed model can be used to identify trade-offs in mobile network configuration to provide capacity and coverage with minimum environmental impact. Given the importance of use stage contribution, reducing the carbon intensity of the electricity consumed by base stations is critical to reducing their global warming potential. However, it is equally important to consider the production stage if the goal is to reduce the use of mineral and metal resources.

Keywords

Base station – Radio access network – 4G-LTE – 5G-NR – Life cycle assessment – Parametric life-cycle model – Teardown – Uncertainty analysis

1 Introduction

Since the turn of the century, the rapid expansion of information and communications technologies (ICTs) has led to intensive development of mobile communication networks connecting mobile terminals to the Internet. On a global scale, Malmodin et al. (2024) estimate that these networks consumed about 161 TWh of electricity and emitted 118 Mt CO_2 eq in 2020, the vast majority of which is due to radio access networks (RANs). Concretely, a RAN is made up of a large number of base stations (BSs) that transmit and receive radio signals to and from mobile terminals and establish connections with the core network. Historical data shows that the energy and carbon footprints of RANs are constantly growing (Malmodin and Lundén 2018; Lundén et al. 2022; Malmodin et al. 2024) and country-wide forecasts predict that they will continue to increase in the future (Bieser et al. 2020; Golard et al. 2023; Stobbe et al. 2023).

Most studies to date have focused on the energy consumption of BSs during their use stage, assuming that it is the hotspot regarding environmental impacts compared to the other life cycle stages. Although this assumption may hold true for the climate change indicator (Scharnhorst 2008; Malmodin et al. 2014), it has not yet been rigorously verified for other environmental impact indicators through a multi-criteria life-cycle assessment (LCA). Furthermore, as mobile data traffic is dramatically growing (Lundén et al. 2022; Ericsson 2024), mobile network operators tend to deploy more small-cell high-capacity BSs operating at lower power levels (Humar et al. 2011; Tombaz et al. 2011), while increasingly relying on renewable energy sources (Lundén et al. 2022). The ensuing acceleration in the pace of technological development is likely to shorten the BS lifetime due to technical obsolescence (Santarius et al. 2022). These trends suggest that impacts of the production stage may become significant in the future. Conversely, the use of recycled materials could reduce the need for raw material extraction and hence reduce the impacts of BS production (Scharnhorst et al. 2006a). This highlights the need for a better understanding of environmental impacts associated with the BS production, which is crucial for informed decision-making in the design and deployment of mobile networks towards sustainability (ITU-T L.1470 2020).

In the literature, the electrical energy consumption of various types of BSs is extensively studied using parametric power models, which are useful for assessing impacts during the use stage. Single-band traditional BSs are analyzed by Jung et al. (2014), Debaillie et al. (2015), and Wang et al. (2017), while legacy multi-band BSs are studied by Lorincz and Matijevic (2014). More advanced systems, such as BSs equipped with massive multiple-input multiple-output (MIMO), are modeled by Desset et al. (2014) and Björnson et al. (2015), and mmWave and THz systems are explored by Desset et al. (2020). These models evaluate both the static and dynamic power consumption of BSs as a function of their traffic load. A recent study by Golard et al. (2024) builds on these previous works to propose an up-to-date parametric power model with realistic numerical parameters estimated by combining on-site measurements with radio equipment documentation. This model estimates that a typical single-band macro-BS consumes around 2 kW on average, corresponding to approximately 5800 kg CO_2 eq per operating year assuming the average electricity grid mix in Europe (Scarlat et al. 2022).

However, the sole consideration of the power consumption of a BS is not sufficient to assess the full environmental impacts of its life cycle. For instance, Humar et al. (2011) demonstrate that the optimal RAN deployment strategy shifts significantly when embodied energy is included in the optimization problem. Despite this, the environmental impacts at other life cycle stages, e.g., the BS production, are much less studied in the literature, with a primary if not exclusive focus on the climate change impact category. Initial research efforts,

like those by Malmodin et al. (2001) and Scharnhorst et al. (2005), assess the production of legacy 2G-GSM BSs, followed by Faist Emmenegger et al. (2006), Scharnhorst et al. (2006a) and Malmodin et al. (2014) for 3G-UMTS BSs. Later, Bergmark (2015) and Ruiz et al. (2022) model BSs supporting 4G-LTE, while Bieser et al. (2020), Ding et al. (2022), Aubet et al. (2024) and Stobbe et al. (2023) provide preliminary LCAs of 5G-NR BSs. Other recent studies focus on specific components for 5G-NR BSs, such as Madon (2021), Kallio et al. (2021) and Guérid et al. (2022).

When it comes to comparing or combining these works, one of the issues is the inconsistency in their scope, e.g., some include the construction of concrete terrace and antenna tower while others focus solely on communication-specific equipment. Similarly, the functional unit (FU) of the LCA studies can vary, e.g., some assess the environmental impact of an entire BS, while others normalize their results per bit of transferred data or per subscriber. As a result, estimates for the production stage vary by an order of magnitude, from 3000 to over 30000 kg CO_2 eq per BS. Excluding construction activities, the most significant impacts typically arise from the manufacturing of electronic components, especially integrated circuits (ICs), and from aluminum production, mainly used in radio units. Another common limitation is the reliance on generic background processes from LCA databases as proxies for BS units due to a lack of specific teardown data, as also pointed out by Bordage et al. (2021), Golard et al. (2023), Stobbe et al. (2023) and Aubet et al. (2024). Additionally, most LCA studies evaluate fixed BS configurations without offering parametric life-cycle models that could be used in optimization problems.

Therefore, this paper introduces a parametric model for assessing the environmental impact of a wide range of BSs over their entire life cycle, according to their technical configuration. The model is intended for use in studies aimed at developing, evaluating, and optimizing RAN deployment strategies, with practical applications in decision-making, eco-design, and sustainability assessments. For instance, it enables comparative analysis between different BS configurations and helps to identify the most environmentally optimal option with respect to network requirements in terms of, e.g., coverage, capacity, energy consumption, etc. The model covers up-to-date commercial BS architectures, i.e., large-scale (macro and micro) cellular BSs emitting from one to hundreds of watts per cell that support multi-band sub-6 GHz technologies for 4G-LTE and 5G-NR communication protocols. Small-scale BSs, such as pico and femto BSs emitting up to 1 W per cell, are not considered in this study as they are not yet fully mature in terms of development and deployment.

This work applies the process-based LCA methodology with an attributional perspective. We focus primarily on the production of the BS (cradle-to-gate LCA) as the modeling of this stage is still rather vague in the literature, while also considering the distribution, use, and end-of-life stages. Given the complexity and heterogeneity of the product system, we employ the modular and parametric LCA approaches as modeling strategies, allowing for a reasonable degree of uncertainty to ensure model flexibility and usability across diverse scenarios. To enable quantitative comparisons between different BS configurations, we provide approximate yet realistic numerical values for the model parameters, including environmental impact factors. These parameters are estimated from an in-depth analysis of the design and hardware composition of BS components based on specific data sources such as detailed teardowns, manufacturer technical documentation, and information from network operators. We then quantify the uncertainty in the model and numerical estimates to enable uncertainty and sensitivity analyses, and to communicate on the accuracy of the results.

This paper is structured as follows. Section 2 outlines the methodology used to develop the model, explaining the LCA modeling strategies and data sources. Section 3 introduces the parametric life-cycle model, first specifying its goal and scope, then detailing the inventory of foreground processes for all BS components, before calculating the corresponding multi-indicator impact factors, and performing the uncertainty quantification. Section 4 applies the proposed model to several BS configurations and interprets examples of results that can be obtained. Finally, Section 5 discusses the limitations of the model and formulates practical recommendations for the users of the model. In addition to this core paper, supplementary information is provided as online resources to detail all modeling assumptions and to fully define the proposed parametric model in order to make it easily usable in future works.

2 Methodology

In this work, we use the process-based LCA methodology defined by the ISO 14040 (2006). In addition, we follow the (widely accepted) recommendation ITU-T L.1410 (2014) on how to apply LCA specifically to ICTs in order to allow other researchers to use this model while ensuring consistency. Accordingly, the BS is an *ICT network good* that can be used as a building block to assess the environmental impacts of *ICT networks* and *ICT services*. Figure 1 shows the system boundaries of our LCA based on the processes considered in ITU-T L.1410 (2014). We exclude from the system boundary *support goods* (e.g., antenna support towers, building, monitoring and security equipment, etc.) and some *support activities* (e.g., maintenance, network operator business activities, etc.) because they are either not strictly necessary for the proper operation of the BS or are not applicable because the BS is considered as an ICT good and not as the service provided by the RAN.

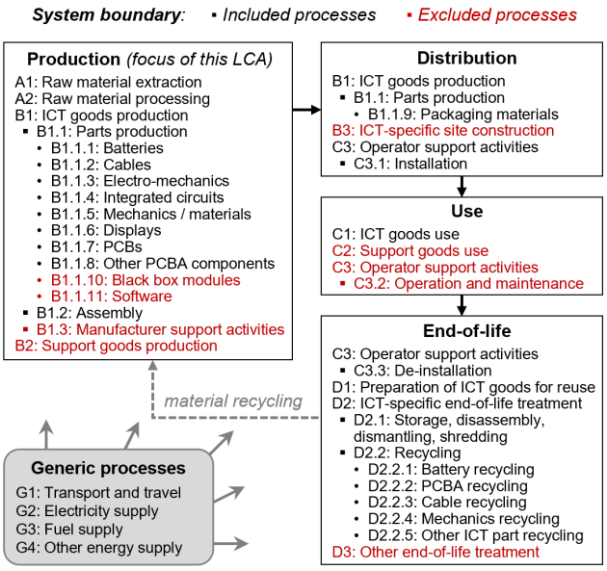

Fig. 1 System boundary for the assessment of a base station according to the recommendation ITU-T L.1410 (2014) with processes grouped into 4 life-cycle stages (slightly adapted from the ITU recommendation)

2.1 Strategies for LCA modeling

A cellular BS consists of 5 types of main components: the baseband unit (BBU) for digital baseband functions, the radio unit (RU) for analog baseband and radio-frequency functions plus signal amplification, the antenna unit (AU) for radio-wave transmission and reception, the power supply unit (PSU) for power conversion

and distribution, and the cables for connecting all these components. The composition of these components varies according to the BS feature configuration. However, conducting an LCA of such a complex and heterogeneous product system is known to be labor-intensive and time-consuming (Scharnhorst 2008). Therefore, we apply two modeling strategies together to simplify the LCA implementation: the *modular* LCA approach and the *parametric* LCA approach, as proposed by Kiemel et al. (2022).

The modular LCA approach involves modeling the product system around reusable elements called modules. Each specific module is first modeled separately, then aggregated together to constitute the whole system (Kiemel et al. 2022). In our model, we define eight modules: we consider five separate modules for the production of each of the five main BS component, to which we add three modules for the distribution, use and end-of-life stages. The modules representing the production of the BBU, RU, AU and cables can be used multiple times for modeling a single BS (i.e., once for each cell), depending on its configuration. Since we consider multiple impact category indicators, the total impact of a BS is represented by a column vector as

$$I_{BS} = \sum_{m=1}^{M} I_m \ ,$$

where M is the total number of BS modules, and I_m is the impact vector of the module m.

The parametric LCA approach aims to model the product system, or its modules, through a set of product-related parameters. This requires determining the functions linking these parameters to the environmental impacts of the system, which often involves regression analysis (Kiemel et al. 2022). In our model, the impact of a foreground process for a given indicator category is the product of its quantity by the corresponding impact factor. These two terms are generally non-linear parametric functions of the set of model variables $x \in X$ defining the BS configuration. The shape and magnitude of these functions are estimated by using regression analysis on specific data sources.

The impact of a module m of the LCA model is then computed by adding together the impacts of its K_m foreground processes. Hence, the column vector of all its impacts is

$$I_m(x) = \sum_{k=1}^{K_m} q_k(x) F_k(x) \ ,$$

where $q_k(x)$ is the parametric quantity of the foreground process k, and $F_k(x)$ is the vector column of its parametric impact factors. It can be rewritten as a matrix product as

$$I_m(x) = \boldsymbol{F}_m(x) Q_m(x)^T \ ,$$

where $Q_m(x)$ is the row vector of all process quantities in the module, and $\boldsymbol{F}_m(x)$ is the matrix resulting from horizontal concatenation of column vectors $F_k(x)$. Note that the units of the elements in any vector $Q_m(x)$ are those used to scale the corresponding impact factors, and may therefore be different (e.g., kg, km, cm², etc.).

2.2 Model variables

The challenge is then to determine *X* the set of *model variables* for the modeling of parametric BS modules. These variables must represent the service provided by the BS in order for the proposed model to be

flexible and easily exploited in next studies. For instance, it should represent features that can be configured by mobile network operators, as well as the operating conditions imposed by network users. As a BS may serve multiple sector and support multiple frequency bands, the first key model variables are the number of sectors N_S and the number of frequency bands N_B. By defining a *cell* as being one frequency band covering one sector, the total number of cells is $N_C = N_S N_B$, e.g., a 3-sectors BS with 2 bands contains 6 cells. Moreover, we identify other key variables that must be defined for each cell such as the carrier frequency, the bandwidth, the number of spatial data layers enabling MIMO, the maximum transmit power per layer, etc. Additional variables are considered for the distribution stage (e.g., the international distribution distance), for the use stage (e.g., the lifetime), and for the end-of-life (e.g., the waste management route). Table 1 provides the complete set of model variables. A similar set of variables is used by Golard et al. (2024) for their parametric BS power model.

Table 1 Complete set of model variables

Scope	Description	Symbol	Unit*	Validity range**
for the whole base station	number of sectors	N_S	#	1-5
	number of frequency bands	N_B	#	1-7
	duration of backup battery at full load	τ_{back}	hours	0-3
	distance between baseband and antenna units	d_{AU}	m	0-50
	distance of international distribution	d_{inter}	km	0-40000
	distance of local distribution	d_{loc}	km	0-1000
	average load of physical resources***	$\bar{l}_{avg}$	/	0-1
	lifetime	L	years	0-20
	source of electricity consumption	-	n.a.	diesel generator, grid or PV system
	route of waste management	-	n.a.	disposal or recycling
for each cell	carrier frequency	f	GHz	0-6
	bandwidth	B	MHz	5-200
	number of spatial data layers	N_L	#	1-8
	maximum transmit power per layer	P_{TX}	W	1-80
	total antenna gain	$G_{TX,dB}$	dBi	0-25
	number of transmit chains	N_{TX}	#	1-64
	number of receive chains	N_{RX}	#	1-64
	relative position of radio unit to baseband unit	δ_{cab}	/	0-1
	duplexing	-	n.a.	FDD or TDD
	communication protocol	-	n.a.	4G-LTE or 5G-NR
	adaptative beamforming	-	n.a.	without or with
	type of antenna unit	-	n.a.	traditional or AAU

* "#" = integer number; "/" = without unit; "n.a." = not applicable

** PV: photovoltaic; FDD: frequency division duplex; TDD: time division duplex; AAU: active antenna unit

*** the load can also be defined for each cell as in Golard et al. (2024)

2.3 Model structure

The general structure of the life-cycle model is shown in Figure 2 by combining the modular and the parametric LCA approaches to compute I_{BS}. Within this framework, we model the impacts of producing the BBU, RUs, AUs and cables that serve one individual cell c by $I_{BBU,c}$, $I_{RU,c}$, $I_{AU,c}$ and $I_{cab,c}$ respectively. These impacts depend on the specific cell configuration defined by the variable subset $X_c \subseteq X$. The impacts of producing the PSU serving all cells of the BS is denoted by I_{PSU}, and the impacts of the distribution, use and end-of-life stages are denoted by I_{dist}, I_{use} and I_{EoL}, respectively. All these terms result from the combination of the *foreground*

process inventory (FPI) with corresponding *impact assessment factors* (IAFs). The goal of this distinction is to bring transparency and flexibility to the model, especially for model users who prefer to employ their own IAFs, e.g., for alternative technologies, alternative operating locations, based on impact factors from another database, etc. Therefore, Section 3 deals separately with the FPI and the calculations of IAFs.

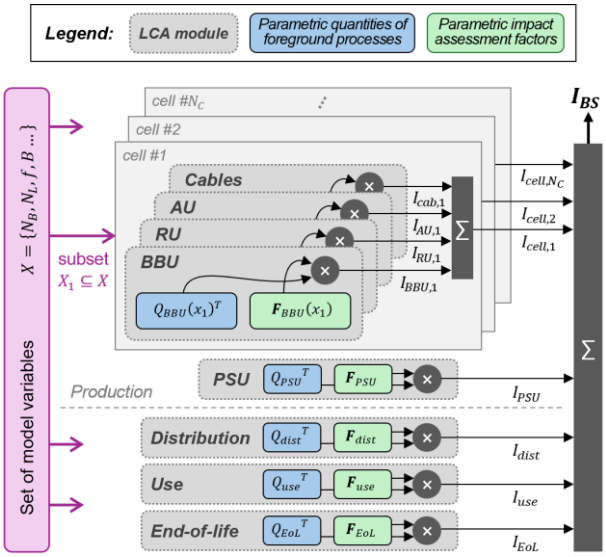

Fig. 2 General structure of the life-cycle model summing the environmental impacts of all parametric life-cycle assessment modules that are each computed by multiplying the foreground process quantities with the corresponding impact assessment factors

2.4 Specific data sources

This LCA study relies on three types of specific data sources: (i) teardowns of BS components, (ii) technical documentation from BS manufacturers, and (iii) data and information from network operators.

Teardowns enable to precisely quantify the material composition of BS components as a function of the BS configuration. However, detailed teardowns are time-consuming to perform and require direct access to the components, with permission to degrade them. We first carried out teardowns of a BBU, a remote RU and a traditional passive AU of a macro cellular BS from the 2010's, supporting several frequency bands, including 4G-LTE at 1.8 GHz with 20 MHz bandwidth and two layers. Figure 3 shows pictures of these disassembled components. Detailed pictures of these teardowns are available in Online Resource 1. In addition, we use a dozen additional teardowns from various external sources covering other BS configurations: from legacy 3G BSs to up-to-date 5G BSs with active antenna units (AAUs) at 3.5 GHz, as well as micro-BSs.

Technical documentation from manufacturers provides a comprehensive description of their BS configuration and related technical specifications. Following recommendations ETSI ES 202 706-1 (2022) and EU 2021/2279 (2021), some manufacturers now provide the dynamic power consumption and bill-of-materials of their products, which is useful for modeling the operating energy consumption, and for complementing the quantification of material composition. In contrast to the teardowns, equipment documentation covers a much wider range of components, with various feature configurations. The drawback of using such secondary data sources is that they sometimes offer less detail than required for in-depth LCA modeling. In this work, we use the

documentation of several hundred pieces of equipment. For confidentiality reasons, the technical documentation cannot be published.

Information and internal data from mobile operators give additional insight into field practices, especially for installation, operation and de-installation of BSs. Knowledge about specific configurations of all the BSs making up a RAN helps to model how the different BS components are configured in practice. For this work, we obtained information and data on the RANs of two main operators in Belgium in 2023. Again, it cannot be published for confidentiality reasons.

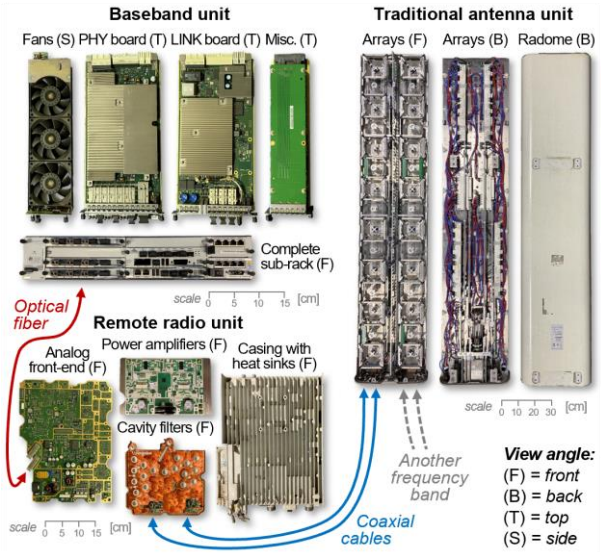

Fig. 3 Pictures of our own teardowns of a baseband unit, a remote radio unit and a traditional passive antenna unit of a macro cellular base station. No teardown of a power supply unit was carried out, and power cables are not shown. Pictures of the different components are not to the same scale

2.5 Numerical estimation of model parameters

Based on the specific data sources, regression analysis is used to determine the shape of all parametric functions of the model and to estimate numerical values of their parameters. Unlike model variables, we consider that the parameters of model functions, referred to as *model parameters*, are fixed by technology and not controlled by network operators nor mobile users (e.g., mass density of BS component casings). Denoting θ the set of model parameters, we can rewrite the process quantity function as $q(x, \theta)$. Then, to estimate θ, we use the data sources comprising D pieces of equipment with feature configurations $\Phi = \{\phi_1, \phi_2 \dots \phi_D\}$ and for which we know the actual process quantities $Y = \{y_1, y_2 \dots y_D\}$. This leads to a non-linear least-squares problem:

$$\hat{\theta} = \arg\min_{\theta} \left\{ \sum_{d=1}^{D} \left(y_d - q(\phi_d, \theta) \right)^2 \right\},$$

that can be solved using numerical methods. The validity of numerical estimation of model parameters is determined by the representativeness of the equipment configurations available in the data sources, which in turn determines the validity range of model variables (given in Table 1). Therefore, we strive to build the specific data sources to match as close as possible the scope of the LCA.

3 Parametric life-cycle model

This section presents the parametric model of the BS life cycle developed according to the methodology described in Section 2. It covers the first three phases of the LCA methodology, namely: (i) the *goal and scope definition*, (ii) the *life-cycle inventory* (LCI) *analysis*, and (iii) the *life-cycle impact assessment* (LCIA). The last part covers the quantification of the uncertainty associated with our modeling and regression analyses.

3.1 Goal and scope

The goal of the proposed model is to enable researchers, mobile network operators and network equipment manufacturers to improve current BS designs, to compare the impacts of different BS configurations, and to support decisions about RAN deployment strategies. The product system represents a macro or micro multi-band sub-6 GHz cellular BS that supports up to several communication protocols including 4G-LTE and 5G-NR. This type of BS provides wireless communication service(s) such as Internet access to mobile users that can be human subscribers or connected objects. The system boundaries include the production, distribution, use and end-of-life stages of all communication-specific BS components, and excludes support equipment and activities. Core network components, data servers and mobile terminals are also excluded from the scope. Given that the BS is parametrically defined, it can provide a variety of services depending on its configuration. We therefore define a parametric FU as *the provision of terrestrial wireless communication services by a BS configured according to the set of model variables* $X = \{N_B, N_L, f, B \dots\}$ *throughout its entire lifetime* L. The corresponding reference flows are highlighted in the product system flow diagram in Figure 4. Variants of the FU can be used by adapting it for one year of use, for a given covered land area, or for a unit of communication service (e.g., one bit of data traffic, one minute of voice calls or one text message). However, the set of model variables does not allow to determine the useful communication service provided by a specific BS, as it would require modeling the radio channel quality between the BS and the mobile users, and then deriving the corresponding spectral efficiency. Yet, in this paper, the service provided by the BS is indirectly represented by its feature configuration in order not to depend on radio channel models that are specific to each BS site.

The LCI analysis involves combining the foreground and background system models (Hauschild et al. 2018). In this paper, we define the *foreground* processes as the main processes of the BS life cycle, for which we seek to establish parametric models. The *background* modeling of these processes consists of informed combination of generic unit processes from the LCA database "ecoinvent version 3.10" (Wernet et al. 2016). Both foreground and background systems are distinguished in Figure 4. The *attributional* modeling perspective is employed implying the use of allocation rules to handle multifunctionality (Hauschild et al. 2018). We therefore use the "allocation, cut-off by classification" system model of ecoinvent (well-known as "cut-off"). In most cases, no allocation procedure is required in the foreground system as most processes deliver separate product flows, except for, e.g., impacts of freight transportation that are allocated by distance and mass of transported product. However, some FU variants may require special allocation procedures, e.g., when the FU focuses on a specific cell or a specific communication service, as further discussed in Section 4.4. Regarding recycling, the allocation of burdens and credits between two successive life cycles is made by applying the same approach as in the ecoinvent cut-off model. It means that no benefits from recycling are allocated to the first life cycle, and the burdens due to recycling process are entirely attributed to the use of recycled materials in the second life cycle

(Wernet et al. 2016). The LCIA results are computed using the multi-indicator LCIA method "Environmental Footprint version 3.1" (EF 3.1) without long-term effects.

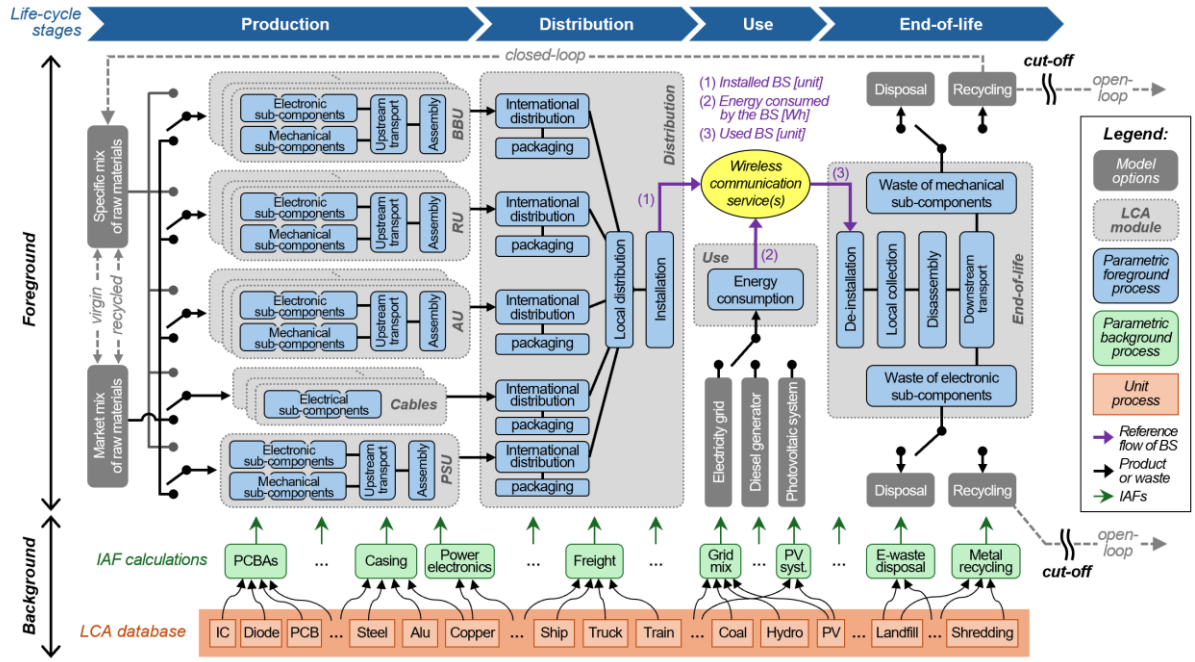

Fig. 4 Flow diagram of the base station (BS) life-cycle model divided into: (i) a foreground system combining parametric foreground processes in several life-cycle assessment (LCA) modules, sometimes depending on specific model options, and (ii) a background system building parametric background processes based on unit processes from a database to calculate impact assessment factors (IAFs)

3.2 Foreground process inventory

The FPI consists in determining the parametric functions of the foreground process quantities that constitute the vector $Q(x)$ for each module of the life-cycle model. This section describes all LCA modules of the BS and their respective modeling in parametric foreground processes. The complete set of foreground processes is provided in Table 2 along with the scaling units to be used when multiplying them by the IAFs. As explained in Section 2.1, the modules representing BBU, RU, AU and cable production can be used multiple times for modeling a single BS. The mathematical expression of all parametric functions with associated numerical parameter estimates are provided in Online Resource 1. This supplementary information also explains the main modeling assumptions and details how regression analyses are performed on the specific data sources.

Table 2 Foreground process inventory

Scope	Module	Description	Parametric functions*	Unit
for each cell	production of the baseband unit	production of the link-layer boards	$e_{link}(x_c)$	cm²
		production of the physical-layer boards	$e_{phy}(x_c)$	cm²
		production of the miscellaneous electronics	$e_{misc}(x_c)$	cm²
		production of the mechanical structure	$m_{BBU}(x_c)$	kg
		upstream transport of the sub-components	$t_{BBU}(x_c)$	kg·km
		final assembly of the component	$a_{BBU}(x_c)$	Wh
	production of the radio unit	production of the power supply	$e_{sup}(x_c)$	cm²
		production of the processing units	$e_{proc}(x_c)$	cm²
		production of the transceivers	$e_{TRX}(x_c)$	cm²
		production of the power amplifiers	$e_{PA}(x_c)$	cm²
		production of the mechanical structure	$m_{RU}(x_c)$	kg
		upstream transport of the sub-components	$t_{RU}(x_c)$	kg·km
		final assembly of the component	$a_{RU}(x_c)$	Wh
	production of the antenna unit	production of the antenna elements	$e_{AE}(x_c)$	kg
		production of the mechanical structure	$m_{AU}(x_c)$	kg
		upstream transport of the sub-components	$t_{AU}(x_c)$	kg·km
		final assembly of the component	$a_{AU}(x_c)$	Wh
	production of cables	production of the optical cables	$e_{opt}(x_c)$	m
		production of the coaxial cables	$e_{coax}(x_c)$	m
		production of the power cables	$e_{pwr}(x_c)$	m
for the whole base station	production of the power supply unit	production of the power converter	$e_{conv}(x)$	kg
		production of the backup batteries	$e_{batt}(x)$	kg
		production of the mechanical structure	$m_{PSU}(x)$	kg
		upstream transport of the sub-components	$t_{PSU}(x)$	kg·km
		final assembly of the component	$a_{PSU}(x)$	Wh
	distribution stage	production and disposal of the packaging	$m_{pack}(x)$	kg
		international distribution of the main components	$t_{inter}(x)$	kg·km
		local distribution of the base station	$t_{loc}(x)$	km
		installation of the base station	$a_{inst}(x)$	Wh
	use stage	energy consumption of the base station	$\epsilon_{cons}(x)$	Wh
	end-of-life stage	de-installation of the base station	$a_{deinst}(x)$	Wh
		local collection of the base station	$t_{col}(x)$	km
		disassembly of the base station	$a_{disas}(x)$	Wh
		downstream transport of the sub-components	$t_{down}(x)$	kg·km
		waste management of the electronic sub-components	$e_{waste}(x)$	kg
		waste management of the mechanical sub-components	$m_{waste}(x)$	kg

* the functions of modules defined for each cell depend on the respective subset X_c of model variables

3.2.1 Modeling approach for the production

The production stage includes raw material acquisition, manufacturing, transport and assembly. As shown in Figure 4, raw materials can be either virgin or recycled. By default, our model assumes that the weighting between these two sources corresponds to the market mix for each material. Another option, which we condition on the adoption of end-of-life recycling, considers the use of a specific raw material mix that contains more recycled material than the market average. Yet specific mixes are limited to materials that can be recycled in a closed loop within the product system, i.e., the metals in mechanical structures but not the materials in electronic components as they require a very high level of purity (Krishnan et al. 2008). The foreground processes involved in the production of main BS components are grouped into four types: the production of electronic sub-

components, the production of mechanical sub-components, the upstream transport of these sub-components from their respective manufacturing factories to the final assembly factory, and the final assembly of the component. In Table 2, we distinguish the four types of process by a specific symbol, respectively e, m, t and a. Notice that these symbols are also used in the other life-cycle stages to identify related processes: t for transport, a for (de-)installation/disassembly, and e and m for waste management of electronic and mechanical sub-components.

To model the production of most sub-components, we scale their quantity according to scaling variables relative to a reference situation. It means that the quantity $q_k(x)$ of a process k is modeled using a reference quantity q_k^{ref} that scales with S scaling variables as

$$q_k(x) = q_k^{ref} \prod_{s=1}^{S} \left(\frac{x_s}{x_s^\star}\right)^{\alpha_{k,s}} ,$$

where the scaling variable s has an actual value x_s, a reference value $x_s^\star$, and a process-specific scaling exponent $\alpha_{k,s}$. We define the reference situation by $f^\star$=1 GHz, $B^\star$=1 MHz, $P^\star$=1 W, $\tau^\star$=1 hour, $\mathcal{M}^\star$=1 kg, and $\mathcal{A}^\star$=1 cm², respectively the reference frequency, bandwidth, power, duration, mass, and surface area. For each foreground process, the model parameters q_k^{ref} and $\alpha_{k,s}$ are estimated as explained in Section 2.5. Yet, to simplify calculations, we restrict scaling exponents to specific values $\alpha \in \{0, 0.25, 0.5, 0.75, 1\}$. A similar scaling approach was previously proposed for BS power consumption models in Debaillie et al. (2015) and Golard et al. (2024).

The modeling approach for transport and assembly processes is the same for all BS components. Due to a lack of primary data, assumptions are needed to model these two types of processes, implying a wider range of uncertainty than relying on specific data sources. Upstream transport is modeled by a mix of freight transportation means for the sub-component mass over the upstream transport distance (in kg·km). Here, the packaging is not modeled as we consider its impacts to be negligible. Assembly is limited to the electricity used for assembling the sub-components into the final BS component, and other assembly processes as well as the construction of the assembly factory are neglected due to lack of information. Manufacturer support activities are outside the scope of this work as mentioned in Figure 1.

3.2.2 Production stage modules

In the BS communication chain, the BBU performs digital functions such as physical resource scheduling, coding, modulation, digital precoding and/or beamforming, decoding, demodulation, etc. (Golard et al. 2024). The BBU is usually made up of a set of boards handling the link and physical layers of communication protocols (Larmo et al. 2009) such as 4G-LTE and 5G-NR. In general, these boards are shared by all BS cells, but specific boards are usually optimized for one given protocol. The BBU boards are hence the electronic sub-components of the BBU which we model by the surface areas of their printed circuit board assemblies (PCBAs). An additional area of PCBA is considered for miscellaneous functions such as power management, fan cooling, etc. The mechanical structure of the BBU includes the mechanical parts of its boards (e.g., front panel, screws, etc.) plus the sub-rack that holds them together, the whole being modeled by its total mass.

Each RU of the BS contains the analog front-end (AFE) and the power amplifiers (PAs) for one cell. The AFE performs specific analog functions in transmission, i.e., digital-to-analog conversion, up-conversion and pre-driving, in reception, i.e., low-noise amplification, down-conversion and analog-to-digital conversion, and for the

whole cell, i.e., frequency synthesis, clock generation and general control. The PAs amplify the radio signals before they are emitted by the antennas (Golard et al. 2024). RUs can be classified into several categories according to two main aspects. The first aspect concerns their transmit power: macro-RUs emits from 40 W to >100 W per cell, compared with 1-40 W per cell for micro-RUs. The second aspect relates to their physical implementation: radio frequency units (RFUs) are installed in the BS cabinet next to the BBU, remote radio units (RRUs) are installed closer to the passive AUs to reduce losses in the cables connecting them together, and active antenna units (AAUs) combine the AFE, PAs and radiating antenna elements (AEs) for one cell into a single physical unit. In this LCA model, the RU module for AAUs includes the production of the AFE and PAs, while the production of the antenna part is modeled by the AU module. In general, a RU can support different communication protocols but are optimized for a specific one (e.g., an AAU at 3.5 GHz is specific to 5G-NR). The AFE and PA functions are performed by electronic sub-components which we distinguish into four parts: the power supply, the processing units, the transceivers (TRXs) and the amplifiers, for which the quantities are once again modeled by the surface area of their PCBA. The mechanical structure of the RU combines a casing with heat sinks to ensure effective heat dissipation. It also supports the cavity filters which are commonly used in RUs for their ability to handle high amounts of power with low losses (Hunter et al. 2002). This whole structure is modeled through its total mass.

The AU radiates the radio frequency signals amplified by the RU and receives the signals emitted by the mobile terminals. A single AU usually covers a unique sector and consists of several two-dimensional antenna arrays, each handling a dedicated frequency band. An antenna array contains multiple AEs arranged in rows and columns and split into sub-arrays. MIMO antennas with multiple sub-arrays are required to implement adaptive beamforming (ABF) (Tahseen et al. 2023). The electronic sub-components of the AU are the AEs comprising all the radiating elements plus the internal cables and the delay lines used to control the delay in radio-frequency signals. The whole is modeled by the total mass. The mechanical structure of the AU consists of a reflective plane which focuses the radiation pattern of the antenna and supports the AEs, plus a radome to protect AEs from outdoor conditions. To compute the mass of this whole structure for one cell, we consider that in traditional "passive" AUs, antenna arrays of different frequency ranges can be superimposed to save space and reduce the wind load, e.g., the frequency bands at 0.8 and 1.8 GHz can be superimposed, but not those at 1.8 and 2.1 GHz (Tahseen et al. 2023). Then, we uniformly allocate the total mass in the full AU per number of supported bands. In contrast, no mass allocation is needed for the so-called "active" AUs as a single AAU supports only one frequency band. In that case, since the mechanical structure of the AU is shared with the contiguous RU, we allocate only the radome to the AU module as the reflective plane corresponds to one side of the RU module.

The PSU supplies power to the BBU and all RUs of the BS. Since the available electrical power source is usually low-voltage alternating current (AC) and as the BS components operate on direct current (DC), the PSU handles AC/DC conversion and power distribution to all BS components (May 2006; Golard et al. 2024). Hence, the first electronic sub-component of the PSU relates to the power conversion and comprises multiple rectifiers, a power distribution panel, a controller, and fans for active cooling. The PSU may also include backup batteries to guarantee a reliable service in case of a power supply failure (May 2006). These two sub-components are modeled by their mass. The mechanical structure of the PSU consists of the complete structure and casing of the BS cabinet plus the sub-rack that houses electronic sub-components of the PSU, the whole being also modeled

through its total mass. Note that the production of additional components required to power isolated BSs with a diesel generator or a photovoltaic (PV) system, e.g., additional storage batteries, converters, etc., is not included in the PSU production module, but rather in the calculation of IAFs for the use stage.

Two types of external cables are required to connect all the BS components together: data cables (i.e., optical fibers and coaxial cables) and power cables. Optical fibers are used to transfer digital data between the physical-layer boards in the BBU and the RUs of corresponding cells. Coaxial cables are then used to transfer the modulated and amplified analog signals between each TRX and the corresponding sub-array in the AU. Power cables carry the electrical power between the PSU and all other active BS components (Denker 2013). The quantity of each cable is modeled with respect to its length, and we consider that the power cables supplying the BBU are already included in the PSU module. As the cables are the end products installed on site, no further assembly nor upstream transport is considered for these components.

3.2.3 Distribution stage module

The distribution stage includes the transport of BS components from their assembly factory to the specific site where they operate, plus their installation on site. The transport is divided in two segments: (i) the international transport between the manufacturer's assembly factory and the network operator's warehouse, and (ii) the local transport between the operator's warehouse and the BS site. The international distribution is modeled by a mix of freight transportation means for the transported mass over the international transport distance (in kg·km) like the upstream transport of sub-components. The mass of each component is calculated by summing the mass of all its sub-components. On top of this, we add the mass of the specific packaging that we no longer consider negligible for worldwide freight. The international distribution distance depends on where the BS components are manufactured and where the operator is based. As with most of today's electronics, we assume that all BS components are manufactured and assembled in East Asia (Yeung 2022). The local distribution is handled by a small truck, the impacts of which are all allocated to the BS as we consider that the entire round-trip is dedicated to the BS installation (and no longer allocated with respect to the mass, as for international freight). The installation of BS components on site consists of manual handling, assembly of mechanical parts, cable connections and system configuration, all carried out by one or more technicians. As for the component assembly, we simply model the BS installation by electricity consumption, with a wide range of uncertainty due to a lack of primary data. We consider that the technicians travel in the same truck as the BS.

3.2.4 Use stage module

The use stage of the BS consists solely of electricity consumption since support activities, e.g., maintenance, are excluded from the scope of the model. Various electricity sources can be used to supply the BS, and our model allows to choose between three typical ones: the electricity grid, a diesel generator, or a PV panel system. The last two options are generally used by isolated off-grid BSs (Malmodin et al. 2018; Malmodin et al. 2024). The instantaneous BS power consumption varies over time depending on the traffic load, e.g., the average BS load is typically lower in the night than in the afternoon (Golard et al. 2023). As this work focuses on the cradle-to-gate modeling and as the literature has already extensively studied the power consumption of various types of BS, we propose to reuse the parametric power model proposed by Golard et al. (2024) to model the BS energy consumption. Indeed, the scope and modeling approach of these authors are very similar to this work (since some authors are the same), in addition to using a similar set of model variables. The total energy consumption of

the BS is calculated over its entire lifetime. Typically, the average hourly load of a BS ranges from 0 to 30% (Golard et al. 2023), but the load profile can evolve over the years with the increase in overall data traffic.

3.2.5 End-of-life stage module

The end-of-life stage is difficult to model because we lack primary data and there is no clear consensus in the literature on the modeling of e-waste management (Ficher et al. 2024). We therefore propose a streamlined modeling approach for this stage. In the following, we only consider the formal waste management of BSs, assuming a 100% collection rate, as they are managed by companies subject to strict e-waste management legislation such as the directive EU 2012/19/EU (2012). The first steps of end-of-life mirror the local part of the distribution stage, i.e., the de-installation of the BS from the site and the local transport back to the operator's warehouse (i.e., the local collection). Next, we assume that all BS components are disassembled and separated into electronic sub-components on one side, and mechanical sub-components on the other. This step is modeled as the counterpart to the assembly of BS components, using the local electricity grid mix. Waste management is assumed to take place in the same region as the BS use, meaning that no international transport is required, but downstream transport is considered and modeled as the upstream transport.

At this point, several waste management routes can be envisaged, such as in Scharnhorst et al. (2006b). We consider that the default route for all BS materials is disposal by incineration and landfill. This is a pessimistic modeling option because no process and associated environmental impacts can be "cut-off" from the product system (e.g., material recovery processes). The other more environmentally friendly route of the model is waste recycling under market capabilities. Indeed, the use of recycled materials in another product system can reduce its production impacts, as shown by Scharnhorst et al. (2006b) for a BS rack. However, assessing recycling using the open-loop substitution approach leads to the invisibilization of recycling processes and a potential underestimation of end-of-life impacts (Ficher et al. 2024). It means that the recycling route, especially in open loop, is an optimistic modeling option. We hence argue that a realistic assessment of the end-of-life lies somewhere between the two options. The impacts of both waste management routes are assumed to be proportional to the mass of waste processed.

3.3 Impact assessment factors

The IAFs contained in vectors $F_k(x)$ are used to compute the environmental impacts associated with each foreground process (see Section 2.1). As shown in Figure 4, IAF calculations rely on background processes built on the unit processes from the ecoinvent database (unit processes are referred to as "dataset" in the ecoinvent documentation). In general, we use the "market for" unit processes to represent the average market composition and to include transport, except when considering specific raw material mixes for which we determine the share of virgin and recycled materials. Due to some limitations in ecoinvent, we additionally develop custom unit processes modeling the production of ICs, connectors, and PAs. The main data sources for building the background processes are teardowns, technical documentation, and bill-of-materials of various BS components. Since these sources lack completeness in relation to the model's validity domain, we assume static IAFs rather than parametric ones, meaning that $F_k(x) = F_k$, which implies additional uncertainty as discussed in Section 3.4.

The rest of this section explains the main assumptions we made to calculate the IAFs and discusses the results shown in Figure 5 for the global warming potential (GWP). An equivalent figure for abiotic resource

depletion potential (ADP) is presented in Online Resource 1. Further details on how we build background processes based on ecoinvent and custom unit processes are also provided in Online Resource 1. The complete list of unit processes used to calculate all IAFs is given in Online Resource 2.

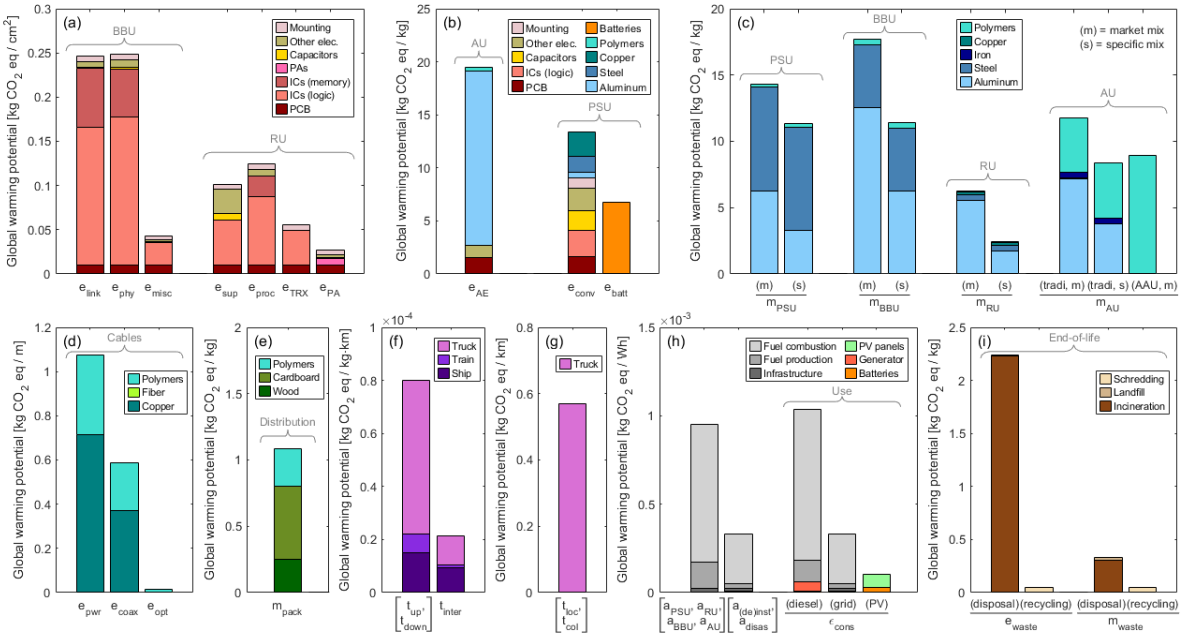

Fig. 5 Global warming potential of all foreground processes for (a) printed circuit board assembly production, (b) other electronic production, (c) mechanical structure production, (d) cable production, (e) packaging production and disposal, (f) freight transport, (g) local transport, (h) electricity consumption, and (i) waste management routes. Some impact factors apply to several processes (in brackets), while other processes may be linked to different impact factors depending on the model options (in parentheses)

3.3.1 Printed circuit board assemblies

A PCBA typically consists of a printed circuit board (PCB) on which active and passive electronic components are mounted. Most of the active components are logic and memory ICs, while the passive components are mainly inductors, capacitors, resistors, and connectors.

We use our own detailed teardowns of a BBU and a RRU to study the composition of their PCBAs. Since these compositions vary significantly depending on the function performed, we calculate specific IAFs for the different types of PCBAs considered in the FPI (see Table 2). For that, we first separate the PCBAs of the BBU (resp. RRU) into three (resp. four) parts according to the function performed by each PCBA region. Then, we list all the electronic components present on these parts and add the PCB mounting processes including the solder paste. Lastly, we allocate all these processes per cm² of PCB surface area. The mass density of PCBAs is estimated around 1 g/cm².

Figure 5(a) shows that the GWP per cm² of PCBAs varies by around an order of magnitude, from 0.03 kg CO_2 eq for providing basic analog functions and up to 0.25 kg CO_2 eq for performing complex digital functions. This difference is explained by a higher density of high-impact components such as digital ICs (for logic and memory) in the link- and physical-layer boards of the BBU. On the other hand, PCBAs performing analog

functions as for TRXs and PAs have a moderate component density to reduce noise and control the impedance of the routing lines (Eastman 1996). Nevertheless, ICs implementing analog functions still have a high manufacturing impact as, e.g., in PAs due to the use of precious metals like gold and silver. The PCBAs supporting power supply and miscellaneous functions have low to moderate impacts on climate change, reflecting a high density of low-impact components (e.g., capacitors, inductors, and small ICs).

3.3.2 Other electronics

Based on our own teardown of a traditional AU, the radiating elements of the AEs are primarily made up of aluminum sheets and polymer parts. The delay lines consist of a non-populated PCB plus a few polymer parts housed in a die-cast aluminum casing. Internal coaxial cables transmit the signal from the external connectors of the AU to the AEs through the delay lines. Whatever the AU type (traditional or AAU), we assume that aluminum sheets are used for all radiating elements below 6 GHz. Moreover, we assume that only primary aluminum is used to manufacture AEs as they presumably need to be of high purity in order not to degrade radio-frequency signals, like other electronic sub-components. Figure 5(b) shows that the aluminum accounts for more than 80% of the GWP of AEs.

The two electronic sub-components of the PSU are modeled using proxies from ecoinvent scaled with respect to their mass, as we could not get a PSU for tearing it down by ourselves. For the power converter sub-component, we chose in ecoinvent the unit process modeling the production of an inverter for a PV system comprising transformers, control units, connectors, etc. Indeed, for a similar rated power magnitude (2.5 kW in this case), we assume a similar composition between an inverter and a rectifier as they perform opposite yet comparable functions (the former converting power from DC to AC, the latter from AC to DC). In Figure 5(b), the impact from copper is due to the wires and the rest to the other electronic components. For the backup battery pack, we consider an even mix of lithium-ion and lead-acid batteries as these two technologies currently coexist in PSUs for BSs. Note that lithium-ion batteries have a higher energy density than lead-acid batteries and thus a higher GWP per kilogram of battery.

3.3.3 Mechanical sub-components

The material compositions of all mechanical sub-components are determined using the teardowns of BS components and equipment documentation from BS manufacturers. During our own teardowns, the different materials were identified based on their appearance, magnetic properties, density, etc. Two types of aluminum are encountered with different manufacturing processes: aluminum sheets and aluminum die-cast parts. The other metals identified are steel, iron and copper. We assume that most of the polymer parts are made of acrylonitrile-butadiene-styrene, and that polyamide is used for glass fiber-reinforced plastic. In all cases, the use of a raw material from the technosphere is coupled with a processing step to produce the desired mechanical element, e.g., injection molding for polymers. The PSU and BBU casings are generally made of steel and aluminum sheets, while the RU casing is made of die-cast aluminum. An internal part of the RU structure is also copper plated for the realization of cavity filters. Conversely, the radome of traditional AUs is made of reinforced plastic to be transparent to radio waves and is mounted on an aluminum structure including the reflective plane. For AAUs, only the radome is considered in the AU since the rest of the structure is shared with the RU and allocated entirely to it (see Section 3.2.2).

As explained in Section 3.2.1, we consider two options for the materials sourcing of mechanical sub-components: a market mix and a specific mix containing more recycled materials. By default, market mixes (as modeled by ecoinvent) are assumed for all materials, and only aluminum can benefit from the option of a specific material mix. The underlying reason is that this option is simple to implement using ecoinvent as a unit process for aluminum scrap recycling is directly available, unlike for other materials. Yet, this limitation is balanced by the fact that aluminum is the material that accounts for most of the GWPs in Figure 5(c), justifying a priority attention. Thereby, we define a closed-loop recycling scenario for aluminum, assuming an optimistic recycling efficiency of 95%. It means that 95% of the aluminum mass in BS components is recovered after recycling to produce a new BS component. The remaining recycling plus manufacturing losses are covered by additional aluminum from the market. Figure 5(c) shows that the higher use of recycled aluminum can reduce the GWP of mechanical structures by one-third to two-thirds compared to the current average mix of raw aluminum.

3.3.4 Cables

As the ecoinvent database lacks granularity and specificity for cable production, we develop specific cable models for the BSs. For the power and coaxial cables, our teardowns help to quantify the mass of main material categories, while their precise compositions are estimated thanks to bill-of-materials disclosed by manufacturers. For the optical fiber cable, a single bill-of-material is used to build the background process. Figure 5(d) shows that the GWP per meter of cables is dominated by copper when it is used, which is the case for coaxial cables and especially power cables. Moreover, there is a difference of two orders of magnitude between the GWP of optical fiber and power cables. In fact, this partly reflects the difference in linear density between all these cables (around 160 g/m, 90 g/m and 4 g/m for respectively the power, coaxial and optical fiber cables).

3.3.5 Packaging and transport

According to equipment documentation from BS manufacturers, the average packaging mass is composed of 55% wooden pallets, 40% corrugated cardboard box and 5% polymers. Yet, cardboard and polymers account for most of the packaging's GWP, as illustrated in Figure 5(e). Upstream and downstream transports are modeled with the same distribution of freight transportation means (per kg·km): 37% truck, 15% train, 24% inland barge and 24% container ship based on (ITF 2022). Using the same approach, the international transport is modeled considering 91% container ship, 7% truck and 2% train based on (Bucsky 2019). In Figure 5(f), the GWP per kg·km of the upstream (or downstream) transport is higher than that of the international transport due to the higher share of road transport. Indeed, road transport has the highest GWP, around 0.16 kg CO_2 eq/t·km, compared to around 0.05 and 0.01 kg CO_2 eq/t·km respectively for rail and container ship. Finally, Figure 5(g) indicates the GWP per km traveled for the local distribution and collection, which is handled exclusively by small trucks entirely dedicated to transporting BS components.

3.3.6 Electricity consumption

The electricity consumed by the final assembly of sub-components is modeled using the medium-voltage electricity grid mix in China, which we assume to represent the electricity mix in East Asia. On the other hand, we consider the European low-voltage grid mix for the electricity used for the installation, de-installation and disassembly of the BS. This therefore applies to a BS deployment in Europe, but we suggest adapting this electricity mix to the specific region of deployment.

Three power supply options are proposed for the use stage energy consumption: the electricity grid (default option), a diesel generator, or a PV panel system. The electricity grid mix in Europe is considered with the same comment as before regarding the location of the BS site. The modeling of electricity grid mixes is directly taken from ecoinvent. For diesel power generation, we include the impacts of producing the generator, producing the fuel, the direct emissions from combustion, and the production of additional batteries. The PV system model includes the production of PV panels and additional batteries. The additional batteries are sized to store up to one and three complete days of BS energy consumption for the diesel and PV systems respectively. We assume the use of lithium-ion batteries only due to their high energy density and long lifetime (Lai et al. 2024). The IAFs for these three options are calculated per Wh of energy consumed, yielding GWPs of around 1000, 950, 330 and 100 g CO_2 eq/kWh for the diesel generator, Chinese grid, European grid and PV system respectively (see Figure 5(h)). As expected, direct emissions dominate the GWP when electricity is partly generated from fossil fuels. GWP is very high when coal is the principal energy source as in China, whereas in Europe more renewable and nuclear energy sources are used in addition to fossil gas (Scarlat et al. 2022). Conversely, the GWP of the PV system is mainly due to the production of PV panels, meaning that impacts per Wh are largely influenced by the power system lifetime, which we assume to be 30 years (hence greater than the BS lifetime).

3.3.7 Waste management

After de-installation, local transport and disassembly, the waste management of electronic and mechanical sub-components is modeled for two different routes. The first route is the disposal by incineration and landfill, for which we estimate the average mass composition of waste from mechanical and electronic sub-components as respectively: 70% aluminum, 10% polymers, and 20% of other materials, and 35% PCBAs, 40% batteries, and 25% cables. To calculate IAFs of the incineration of these wastes plus the following landfill of residues and bottom-ash, we use the unit processes in ecoinvent that correspond (or at least are the closest) to the specific waste compositions. As ecoinvent still considers the recycling of some residues after incineration (and hence cut them off), we add their landfill to the IAF calculations. The second waste management route is recycling by first shredding the waste, of which 95% is then available for material recovery (and hence cut-off) and 5% is lost and landfilled. The recycling routes of both types of waste are modeled in the same way considering waste shredding plus the landfill of the few losses. Figure 5(i) shows that most of the GWP of disposal comes from the incineration. The GWP of e-waste incineration is also greater than for waste of mechanical sub-components because they contain more materials to burn and thus emit more greenhouse gases compared to, e.g., metals. For both types of waste, the impact of preparing materials for recycling is mainly due to shredding, and is at least one order of magnitude lower than that of disposal.

3.4 Uncertainty quantification

According to Heijungs (2024), the uncertainty of LCA results stems from two main aspects: the *variability* (e.g., in process quantities, between years, between manufacturers, etc.) and the *error* (e.g., in the use of proxies to calculate IAFs, in the model structure, due to a lack of primary data, etc.). In this section, we do not aim to conduct a comprehensive uncertainty analysis (i.e., from quantitative temporal variability to qualitative epistemological uncertainty as articulated by Hauschild et al. (2018)), but rather to give a quantitative indication of the uncertainty in the model and numerical estimates. Furthermore, we only address the uncertainty that is

specific to our model, i.e., related to the FPI and IAF calculations, but we do not cover the additional uncertainty in the LCI of ecoinvent and from the EF 3.1 method.

So far in the paper, we only talked about deterministic point estimates that are supposed to represent "typical" or "most representative" values. Now, we introduce a stochastic dimension in the model to capture the quantitative uncertainty which is mathematically represented by a probability density function. What we do in practice is to represent every foreground process quantity and IAF vector (i.e., $q(x)$ and $F(x)$) by a lognormal distribution for which we set the median to be the deterministic point estimate and we determine the geometric standard deviation (GSD) to reflect the associated stochastic uncertainty. As an example, a GSD of 1.40 corresponds to a lognormal distribution with an interquartile range (IQR) from -20% to $+25\%$ relative to the median. The choice of lognormal distribution is motivated by three reasons: (i) it is positive definite which is consistent for process quantities and IAFs, (ii) it allows to analyze order-of-magnitude variations rather than symmetrical variations, and (iii) it fits well with the empirical variability observed in the specific data sources. The overall uncertainty in LCIA results is calculated using Monte Carlo simulations (Hauschild et al. 2018; Heijungs 2024) with 10000 random generations. Such simulations facilitate mathematical operations on stochastic uncertainties and ease the uncertainty propagation between linked parametric processes, e.g., the uncertain mass of a BS component influences the transport quantity, which is itself uncertain even for a known transported mass.

To calculate the GSD of lognormal distributions, we use the NUSAP scheme (acronym for Numeral, Unit, Spread, Assessment and Pedigree) that aims at expressing and communicating uncertainties in numerical information (Heijungs 2024; Funtowicz and Ravetz 1990). For each foreground process quantity and IAF vector, we first apply the *spread* step by calculating the related variability in the specific data sources when enough data are available. Next, in the *assessment* step, we determine an additional quantitative uncertainty factor expressing the degree of confidence we have in the numerical value and its spread. This is intended to give an idea of the magnitude of the potential error that could be made by the model, based on our own judgments. The final qualitative *pedrigree* step is not performed in this work. The total uncertainty factor is calculated by combining the uncertainty factors of the spread and assessment steps as in Limpert et al. (2001), assuming independent lognormal distributions.

Table 3 Uncertainty factor for the foreground process inventory (FPI) and impact assessment factors (IAFs) expressed in geometric standard deviation

(Type of) foreground process	FPI			IAFs
	variability	error*	total	error*
electronic sub-component production	1.41	1.12	1.44	1.44
mechanical sub-component production	1.41	1.12	1.44	1.80
upstream/downstream transport	-	3.16	3.16	1.80
distribution and collection transport	n.a.	n.a.	n.a.	1.17
(dis)assembly and (de-)installation	-	3.16	3.16	1.17
energy consumption (in use stage)	1.25	1.12	1.28	1.17
waste management routes	-	1.41	1.41	3.62

* based on our own judgments

Table 3 provides the uncertainty factors expressed as GSD for the FPI and IAFs per (type of) foreground process. These factors are presented separately for the variability (from the spread step) and the error (from the

assessment step). FPI variability factors for processes for which no primary data source is available (e.g., assembly) cannot be calculated, leading to higher error factors. Similarly, we cannot calculate variability factors for IAFs because they are mainly calculated based on a single teardown. Instead, IAF error factors capture the expected variability of process composition plus the confidence we have in our modeling choices for building the background processes based on ecoinvent. Uncertainty quantification does not apply for the distribution and collection transport at the FPI level as these are input variables to the model. Online Resource 1 provides more details on how the uncertainty factors are calculated.

4 Results and interpretations

This section applies the proposed parametric model to various scenarios in order to demonstrate the results it can produce and highlight its flexibility. At the same time, we conduct the final phase of the LCA, i.e., the *interpretation of results* with the aim of supporting BS eco-design and decision-making about RAN deployment for reducing their environmental impacts.

Table 4 Typical base station configurations

Variable	3-bands*			2T2R	8T8R	64T64R	micro-4T4R	micro-16T16R
N_S	3			3	3	3	3	3
N_B	3			1	1	1	1	1
τ_{back} [hours]	0.25			0.25	0.25	0.25	0.25	0.25
d_{AU} [m]	25			25	25	25	10	10
d_{inter} [km]	20000			20000	20000	20000	20000	20000
d_{loc} [km]	500			500	500	500	500	500
$\bar{l}_{avg}$	0.1			0.1	0.1	0.1	0.1	0.1
L [years]	10			10	10	10	5	5
electricity source	diesel gen. (or PV)			grid	grid	grid	grid	grid
waste management	disposal (or recycling)			disposal	disposal	disposal	disposal	disposal
f [GHz]	0.8	1.8	2.6	1.8	3.5	3.5	1.8	3.5
B [MHz]	10	20	20	20	100	100	20	100
N_L	2	2	4	2	8	8	4	8
P_{TX} [W]	40	40	20	40	25	25	5	2.5
$G_{TX,dB}$ [dBi]	16	16	16	16	20	23	7	14
N_{TX}	2	2	4	2	8	64	4	16
N_{RX}	2	2	4	2	8	64	4	16
δ_{cab}	0.8	0.8	0.8	0.8	0.8	1	0.8	1
duplexing	FDD	FDD	FDD	FDD	TDD	TDD	FDD	TDD
protocol	4G-LTE	4G-LTE	4G-LTE	4G-LTE	5G-NR	5G-NR	4G-LTE	5G-NR
ABF	without	without	without	w/o	with	with	w/o	with
AU type	tradi.	tradi.	tradi.	tradi.	tradi.	AAU	tradi.	AAU
capacity [Mbps]	80+160+320 = 560			160	3200	3200	320	3200
coverage [km²]	min(52.6, 7.7, 2.6) = 2.6			7.7	1.1	1.7	0.4	0.1

* illustrative base case for the result interpretation (in parentheses = options for an alternative configuration)

4.1 Base station configurations

In Table 4, we provide six examples of typical BS configurations to illustrate the rest of this section. The first four configurations correspond to macro-BSs and the last two are micro-BSs. They all have three sectors. The first configuration is the only one to support more than one frequency band. This serves as illustrative base case, as this configuration is very common in mobile networks. All other single-band configurations enable finer

comparisons when changing other variables than the number of bands. These configurations can be combined to obtain more sophisticated BS configurations. Half of the configurations operate with the 4G-LTE protocol, and the other half with 5G-NR. The latter use the 3.5 GHz band in TDD with a bandwidth of 100 MHz, and their AUs always feature ABF. AAUs are used when the number of TRXs is greater than 8. An alternative version of the 3-bands configuration is used to analyze the effect of recycling, as well as the switch of power supply from a diesel generator to a PV system. In all other cases, no recycling is considered, and electricity is supplied from the grid, assumed to be the average mix in Europe. The lifetime of macro-BSs is set at 10 years, and that of micro-BSs at 5 years. We also assume an average physical load of 10%, which is shown to be realistic by Golard et al. (2024). However, we consider that no power-saving features (e.g., sleep modes) are implemented, which means that most of the energy consumption comes from the static power consumption of the BS. Moreover, the two last rows of Table 4 provide the data throughput capacity and the coverage area of each BS configuration. These are calculated by considering a realistic spectral efficiency of 4 bps/Hz and by applying the modified "COST231-Hata" radio channel propagation model given by Khan (2009) in an urban scenario. Details of related calculations are given in Online Resource 1.

4.2 Assessment of the production stage

As the model primarily focuses on the production stage, we first examine in Figure 6(a) the impacts of this stage alone in the illustrative 3-bands configuration. A quick hotspot analysis reveals that the RUs dominate most impact categories, often followed by the AUs. This reflects the high number of these components, which is directly related to the number of BS cells. Power cables impact strongly on certain categories because of the substantial amount of copper they contain. Impacts of electronic sub-components are mainly due to PCBA manufacturing (especially the ICs), and those of mechanical sub-components to aluminum production. Upstream transport and final component assembly are clearly negligible in all impact categories.

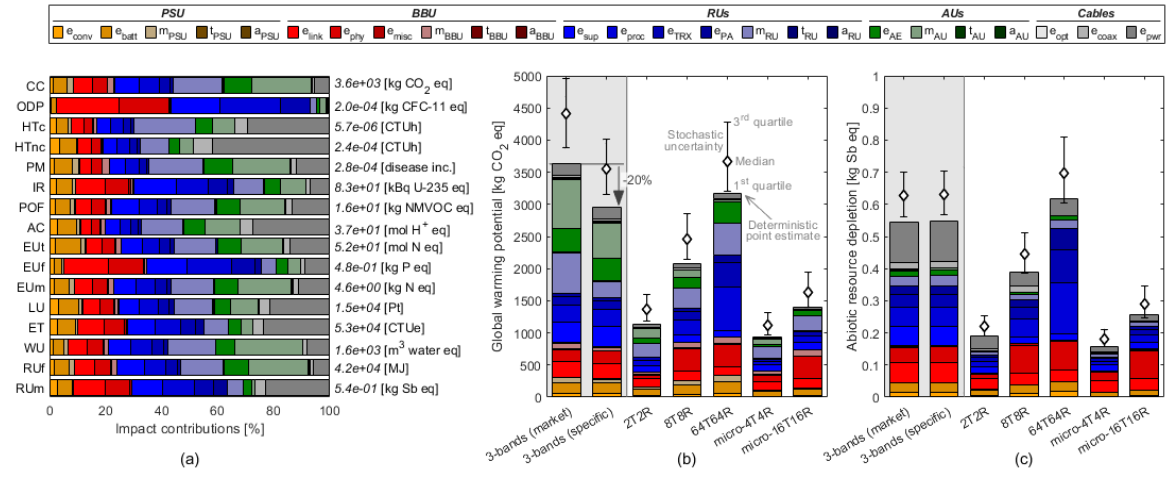

Fig. 6 Results of the production stage (a) in the 3-bands configuration for all Environmental Footprint categories: climate change (CC), ozone depletion (ODP), human toxicity – cancer (HTc) and – non-cancer (HTnc), particulate matter (PM), ionizing radiation (IR), photochemical ozone formation (POF), acidification (AC), eutrophication – terrestrial (EUt), – freshwater (EUf) and – marine (EUm), land use (LU), ecotoxicity freshwater (ET), water use (WU), and resource use – fossils (RUf) and – minerals and metals (RUm), and in all typical base station configurations (b) for the global warming potential, and (c) for the abiotic resource depletion potential

Figure 6(b) focuses on the climate change impact category but extends the results to all typical BSs configurations. This illustrates how the proposed parametric model can be used to compare different BS configurations. Among all greenhouse gases, carbon dioxide accounts for around 85% of the GWP (see Online Resource 1), the remainder being due to methane emissions from fossil fuels as well as fluorinated gases needed for electronics manufacturing (Hess 2024). In the 3-bands scenario, the use of mainly recycled aluminum (in a closed loop with a recycling rate of 95%) reduces the GWP of BS production by 20% compared to the use of aluminum from the market. In single-band scenarios, the deterministic GWP of macro-BSs production lies between 1000 and 3500 kg CO_2 eq, which is in most cases higher than for micro-BSs, in the range of 1000-1500 kg CO_2 eq. This is due to higher transmit power requiring larger RUs and PSUs, and to higher antenna gain implying more AEs and hence larger AUs. Similarly, for a given cell size, multiplying the number of TRXs increases the required PCBA area in RUs, as well as the number of AEs in the AU. The bandwidth and the number of layers (and thus the BS capacity) rather influence the GWP of BBU production. Finally, using AAUs instead of traditional AUs reduces the impact of the mechanical part of AUs.

Figure 6(c) shows the ADP results, i.e., the indicator of the "resource use – minerals and metals" category, as an example of another impact category revealing quite different trends. Overall, variations between BS configurations are like those observed for GWP, except that no savings are obtained from the use of more recycled aluminum because of other critical resources used in the metallurgical recycling processes. The major change lies rather in the contributions of foreground processes. Compared to the GWP, the contribution of mechanical structure production is lower for ADP, reducing the AU contribution to a small fraction, while that of PCBA and power cable production increases, particularly due to copper and gold.

In addition to deterministic results, uncertainty ranges are also displayed in Figure 6(b) and Figure 6(c) through the IQRs and medians of the stochastic assessments. We can then be surprised by the fact that the medians of stochastic assessments are roughly 20% higher than the deterministic point estimates, and that the latter are sometimes even below the first quartile of stochastic assessments. In fact, this is due to the positive skewness of the lognormal distributions that are summed to calculate the total impacts. Thus, another important result is that neglecting uncertainties could result in underestimation of potential environmental impacts. To carry out uncertainty and sensitivity analyses, we propose to use a common rule of thumb stating that a difference between two configurations can be considered significant when their IQRs do not overlap, as further discussed in Heijungs (2024). In this perspective, the difference between production impacts for 64T64R and micro-16T16R configurations is significant, whereas this is not the case between 2T2R and micro-4T4R BSs. Furthermore, the high uncertainty in upstream transport and final assembly (see Table 3) is not strongly reflected in the overall uncertainty due to their very small relative contribution.

4.3 Comparison between life-cycle stages

Including LCA modules for distribution, use, and end-of-life allows for direct comparison across all life-cycle stages. Figure 7(a) shows the GWP results per life-cycle stage in all typical BSs configurations and Figure 7(b) focuses on ADP. Note that the y-axis is in logarithmic scale.

Regarding climate change, the use stage is clearly the hotspot. For macro-BSs, it accounts for more than 90% of the total GWP, except when powered by a PV system for which the carbon intensity is ×3 and ×10 lower

than the electricity grid and the diesel generator, respectively. In any case, the GWP of the production stage never exceeds 15% of the total carbon footprint, even in the case of micro-BS. This shows that decarbonizing the electricity supply is the main lever for reducing the total carbon footprint of a BS. However, power-saving features are neglected in these results, and we can therefore expect their implementation to increase the share of the production stage in total BS GWP, making this stage non-negligible in RAN deployment strategies. Recycling also reduces the GWP of production and end-of-life stages to a lesser extent. Regarding ADP, the production stage is another hotspot, accounting for up to 60% of the total impact of micro-BSs. Contrary to GWP, powering BSs with a PV system is ×3 more mineral and metal resource intensive than with a diesel generator, and ×2 more than with the electricity grid (which is dominated by the copper in distribution networks). For all typical configurations, distribution and end-of-life stages are largely dominated by local transport (see Online Resource 1) and do not contribute much to the total environmental impacts of BSs.

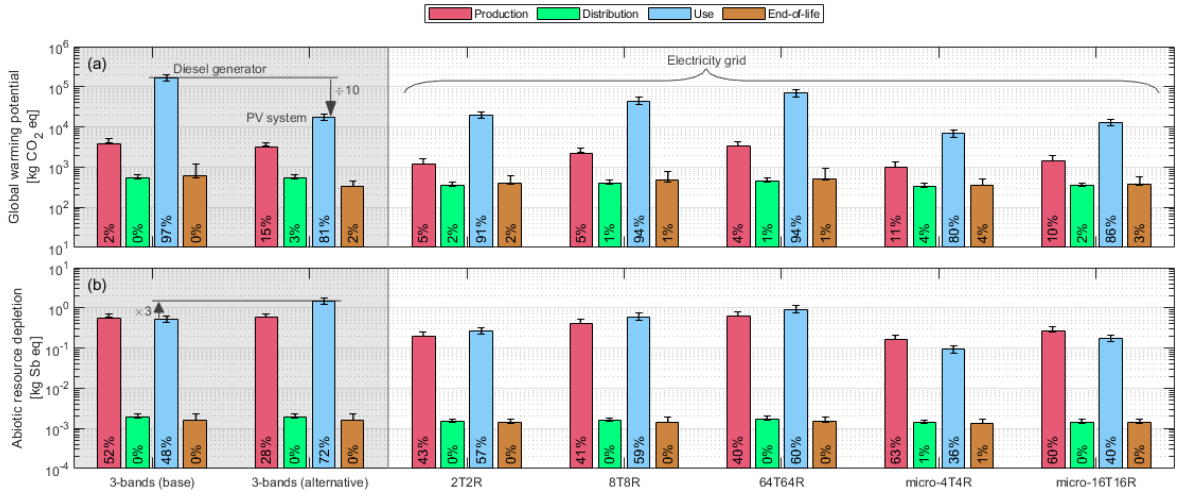

Fig. 7 Results by life-cycle stage in all typical base station configurations (a) for the global warming potential, and (b) for the abiotic resource depletion potential. For the sake of clarity, only the uncertainty IQR is displayed and not the median

4.4 Influence of the functional unit definition

In this section, we aim to analyze how a change in the definition of the parametric FU influences the results and related findings. Figure 8 shows the total life-cycle GWP in all typical BS configurations, considering two examples of FUs: in Figure 8(a) the *provision of all communication services by the whole BS over its entire lifetime* (as before), and in Figure 8(b) the *provision of one Mbps of data throughput capacity over one km² of coverage area during one operating year*. In the latter case, the total impact of the BS is uniformly allocated per FU. Moreover, the two most impacting and less impacting configurations (namely the *worst* and *best* configurations) are highlighted for each FU.

By comparing the obtained results, clear differences in trends appear between the two FUs. For example, the 64T64R BS is one of the worst configurations with the first FU and concurrently one of the best with the second FU thanks to its very high capacity. The opposite occurs with the micro-4T4R configuration due to its small coverage, short lifetime and low capacity. The emerging findings would be that deploying more and more small-scale BSs is not the best choice according to the second FU, even if their absolute GWPs per BS are the

lowest with the first FU. On the contrary, the use of low-carbon electricity seems to be a good option for both FUs. Yet, other trends may emerge for other impact categories. Therefore, when comparing different BS configurations, the definition of the FU strongly influences the results and findings. It is thus of crucial importance to define a FU that suits the goal of the LCA with regard to the key services provided by the studied BSs.

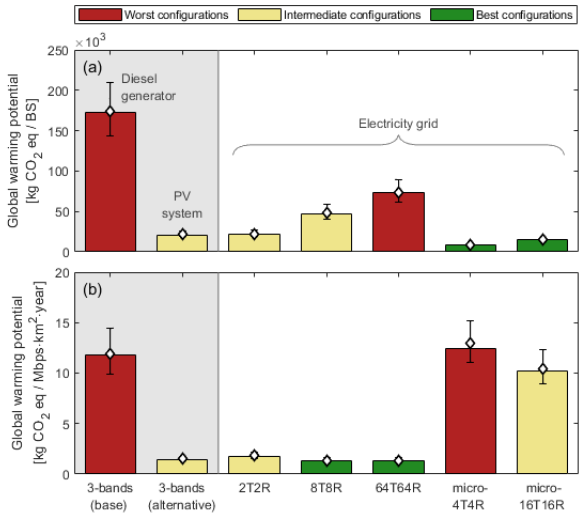

Fig. 8 Total global warming potential in all typical base station configurations for two different functional units: (a) for the whole base station over its entire lifetime, and (b) for a given unit of communication service

5 Discussion

Comparing our results with previously published LCAs, we find the same conclusion that the use stage dominates the impact on climate change. Yet our GWP estimates for BS production are rather at the low end of the assessment range. This can be explained by the exclusion from the scope of support goods as well as the construction of site facilities. Besides, no source allows us to compare our results for the other impact categories. The rest of this section discusses the limitations of the proposed parametric model. Then, it formulates some practical recommendations on how to use it.

5.1 Limitations

A major limitation of the model lies in the amount of specific and primary data sources, which affects its technological, geographical and temporal representativeness. This also prevent the model from capturing variability in the foreground and background systems over time, across manufacturers, and between technologies. Less information is also available for recent BS designs such as AAUs and micro-BSs. These issues justify limiting the LCA scope to macro and micro sub-6 GHz BSs. In addition, certain assumptions in the FPI deserve to be validated (e.g., the power consumption of final assembly and installation), even if they appear to be negligible. At the background system level, the use of a small number of teardowns for IAF calculations impedes a comprehensive view of the sub-component compositions. This led us to consider static IAFs only, whereas they would actually vary, e.g., depending on the production year. Moreover, IAF calculations rely on ecoinvent which generally lacks geographical and technological granularity to perfectly match the background processes, leading to the prevalent use of global average unit processes and the development of custom unit processes.

Other limitations relate to methodological choices and to the structure of the model. First, to account for the heterogeneity of BS components, we propose a modular approach in which certain modules are defined for individual cells. This modeling choice implies that the BS is perfectly sized with respect to the model variables and especially the number of cells. In practice, however, BSs may be oversized to allow for later network upgrades. Second, the use of the cut-off perspective does not provide any benefit for recycling, which strongly favors the use of secondary materials but does not incentivize waste producers to maximize waste recycling (Wernet et al. 2016). The associated "100:0 approach" for recycling burden allocation clearly favors the first user of a material, to the detriment of the second user of the recycled material. This weighting could be adapted to be within a range of 80:20 to 20:80 to comply with EU 2021/2279 (2021), but this would require the use of another LCA database than ecoinvent. Third, we could have considered other specific raw material mixes in addition to aluminum such as for electronics and polymer production. However, this would require a more detailed analysis of waste management routes, as well as the provision of the associated specific processes in the databases. For the same reason, end-of-life modeling remains highly streamlined.

To partly address these limitations, we quantify the uncertainty associated with the model and numerical estimates in Section 3.4, which in turn enables uncertainty and sensitivity analyses. We believe this step is essential to evaluate and communicate on the accuracy of LCA results and conclusions.

5.2 Practical recommendations

The proposed BS model can be used as a building block to study larger product systems such as *ICT networks* and *ICT services*, defined by ITU-T L. 1410 (2014) as logical structures physically made up of *ICT goods* and relying on building premises, civil works to create cable ways, air conditioning, etc. These additional products must therefore be modeled alongside the BS. Similarly, if the BS model is used to study the upgrade of an existing RAN, it may not be necessary to include all the LCA modules within the scope of the study. For instance, we could imagine that the addition of a frequency band on an existing site could be limited to the deployment of RU and AU components with a reuse of existing cables, BBU and PSU.

This reasoning can also lead to questions like "how to allocate the impacts of shared infrastructure between several BS?" or "should we also attribute to a new BS a share of impacts from the previous construction of the pylon and other site facilities?". In fact, this raises the question of whether the *consequential* modeling perspective is more appropriate in some cases than the *attributional* one. In this context, we note that "while the background system is modeled differently in attributional and consequential LCA, the foreground system is overall modeled in the same way" (Hauschild et al. 2018). This means that, thanks to the flexibility of our BS model, it would be correct for a consequential LCA to keep the same FPI as proposed and simply recalculate the IAFs on the basis of marginal (and no longer average) environmental impacts. We leave it up to the model's users to decide how to deal with these issues but draw attention to the need to treat them carefully.

If the intended use of the BS model is to inform decisions about future BS deployments, model's users also need to look at emerging technologies whose level of development may be at different stages, depending on how far into the future the study is carried out. In this case, the principles of *prospective* LCA proposed by Arvidsson et al. (2017) should be applied, i.e., prospective modeling of both foreground and background systems, as well as including technology alternatives that go beyond the current state-of-the-art. Again, the inherent

distinction between FPI and IAFs enables the BS model to be adapted to such a prospective LCA. For instance, we could modify numerical parameters of the FPI by envisioning technical improvements, e.g., a reduction in PCBA surface area in the reference situation. At the same time, the technosphere may evolve in such a way as to modify the background model, implying a recalculation of IAFs, e.g., for electricity grid, for IC manufacturing, considering a higher proportion of recycled materials on the market, etc.

Finally, we remind that LCA serves to evaluate the *eco-efficiency* of the product system according to an established FU (Hauschild et al. 2020). While this relative perspective helps to reduce the environmental impacts of the BS, it does not assess whether these impacts are sustainable or not with respect to the planetary boundaries (Richardson et al. 2023). Within this context, the *absolute sustainability* approach must be adopted by considering allocation principles to share the safe operating space (Hjalsted et al. 2021) in order to identify which portion of this space can be allocated to, e.g., the RAN.

6 Conclusion

This paper presents a model for assessing the environmental impacts of a BS providing wireless communication services. The entire life cycle is covered, from the acquisition of raw materials for manufacturing the BS components to their management at the end-of-life, with a primary focus on the production stage. The model is based on the modular and parametric LCA approaches, enabling the model to be adapted to different BS configurations. The intended use of the model is to assist in the eco-design of BSs and to support decision-making about RAN deployments. The model is hence configurable with respect to multiple variables representing the features and options controlled by network operators as well as the operating conditions imposed by the users. The model is structured into a foreground and a background system, offering a high degree of flexibility. The former inventories the foreground processes for which we propose parametric functions that model their quantities in all modules of the model. The latter builds background processes based on the ecoinvent database to calculate impact factors using the multi-criteria LCIA method EF 3.1. In addition, we estimate realistic numerical values for the model parameters on the basis of specific data sources. This enables quantitative comparisons between different BS configurations. We therefore hope that this BS model will be used by other researchers in next studies.

Afterwards, the model is applied to six typical BS configurations, ranging from single-band macro-BSs in 4G-LTE to micro-BSs supporting massive-MIMO in 5G-NR, as well as a multi-band BS. The results show that for the climate change category the use stage largely dominates the other life-cycle stages regardless of the electricity source, ranging from 80% to >95% of the total GWP over the entire life cycle. Production is the second stage with the largest impact on climate change, while the distribution and end-of-life stages are negligible. The GWP of the production stage varies fourfold between all typical configurations, i.e., from 1000 to 4000 kg CO_2 eq, mainly due to the production of electronic sub-components. Conversely, an analysis of the ADP shows that the production stage can dominate the use stage in certain BS configurations, accounting for between 30% and 60% of the total impact, the other two stages remaining negligible. Moreover, sub-component contributions to production impacts vary according to impact category. This shows why a multi-indicator analysis is necessary to avoid burden-shifting between life-cycle stages and BS components. We also point out that the definition of the FU influences the conclusions drawn when comparing different BS configurations. For instance, if we consider the entire life cycle of one BS unit, micro-BSs always have a lower GWP than macro-BSs. However, if we modify

the FU to consider the services provided to users in terms of network coverage and data throughput capacity, then the results of the study are more in favor of macro-BSs.

To communicate the uncertainty in the proposed model and numerical estimates, we first quantify the variability associated with our regression analyses on specific data sources. Next, we assess the modeling error according to our own judgment, and we combine both together to obtain uncertainty factors. This enables us to estimate the range of stochastic results using Monte Carlo simulations. The resulting IQR of uncertainty is ±20% around the median. We further observe that the deterministic point estimates of production stage impacts underestimate by about 20% the same results calculated stochastically, taking uncertainty into account. This is due to the positive skewness of lognormal distributions used to model uncertainty.

Finally, regarding the current industry trends, we identify that the most effective lever for reducing the GWP of BSs is to reduce the carbon intensity of the electricity they consume during their use stage, whereas to reduce the ADP it is equally important to apply measures at the production stage like reducing the use of copper and gold. Besides, efforts to maximize the use of recycled aluminum for manufacturing the BS, and the complete BS recycling at the end-of-life, have little to no influence on reducing the total GWP and ADP. Furthermore, the trend towards increasing the BS capacity leads to an increase in the total GWP per BS, while the trend towards developing BSs with reduced coverage to densify the RAN results in a reduction of the total impact per BS. At the scale of a complete RAN, there is therefore a trade-off to achieve in terms of BS configurations to provide capacity and coverage with minimum environmental impacts.

References

Arvidsson R, Tillman AM, Sandén BA, Janssen M, Nordelöf A, Kushnir D, Molander S (2018) Environmental assessment of emerging technologies: Recommendations for prospective LCA. J Ind Ecol 22(6):1286-1294. https://doi.org/10.1111/jiec.12690

Aubet L, Rabot A, Bitard L, Riolo C (2024) Empreinte environnementale de la fourniture d'accès internet en France. ADEME. https://librairie.ademe.fr/industrie-et-production-durable/6789-evaluation-de-l-empreinte-environnementale-de-la-fourniture-d-acces-a-internet-en-france.html. Accessed 15 October 2024

Bergmark P (2015) Life cycle assessment of an LTE base station based on primary data. Third ETSI Workshop on ICT Energy Efficiency and Environmental Sustainability. https://docbox.etsi.org/workshop/2015/201506_EEWORKSHOP/SESSION03_LCA/LCA_of_LTE__based_station_primary_data_Bergmark_Ericsson.pdf. Accessed 15 October 2024

Bieser J, Salieri B, Hischier R, Hilty L (2020) Next generation mobile networks: Problem or opportunity for climate protection? University of Zurich, Empa. https://doi.org/10.5167/uzh-191299

Björnson E, Sanguinetti L, Hoydis J, Debbah M (2015) Optimal design of energy-efficient multi-user MIMO systems: Is massive MIMO the answer? IEEE T Wirel Commun 14(6):3059-3075. https://doi.org/10.1109/TWC.2015.2400437

Bordage F, de Montenay L, Benqassem S, Delmas-Orgelet J, Domon F, Prunel D et al. (2021) Digital technologies in Europe: An environmental life cycle approach. GreenIT.fr. https://extranet.greens-efa-service.eu/public/media/file/1/7388. Accessed 15 October 2024

Bucsky P (2019) The iron Silk Road: How important is it? Area Dev Policy 5(2):146–166. https://doi.org/10.1080/23792949.2019.1672571

Debaillie B, Desset C, Louagie F (2015) A flexible and future-proof power model for cellular base stations. IEEE 81st Vehicular Technology Conference (VTC Spring). https://doi.org/10.1109/VTCSpring.2015.7145603

Denker M (2013) Remote radio head systems – Requirements and concept of lightning and overvoltage protection. 35th International Telecommunications Energy Conference, Smart Power and Efficiency (INTELEC). https://ieeexplore.ieee.org/document/6663274

Desset C, Debaillie B, Louagie F (2014) Modeling the hardware power consumption of large scale antenna systems. IEEE Online Conference on Green Communications (OnlineGreenComm). https://doi.org/10.1109/OnlineGreenCom.2014.7114430

Desset C, Wambacq P, Zhang Y, Ingels M, Bourdoux A (2020) A flexible power model for mm-wave and THz high-throughput communication systems. IEEE 31st Annual International Symposium on Personal, Indoor and Mobile Radio Communications (PIMRC). https://doi.org/10.1109/PIMRC48278.2020.9217264

Ding Y, Duan H, Xie M, Mao R, Wang J, Zhang W (2022) Carbon emissions and mitigation potentials of 5G base station in China. Resour Conserv Recycl 182:106339. https://doi.org/10.1016/j.resconrec.2022.106339

Eastman NL (1996) Considerations for mixed analog/digital PCB design. Wescon. https://doi.org/10.1109/WESCON.1996.554004

Ericsson (2024) Ericsson Mobility Report June 2024. Ericsson Report. https://www.ericsson.com/49ed78/assets/local/reports-papers/mobility-report/documents/2024/ericsson-mobility-report-june-2024.pdf. Accessed 15 October 2024

ETSI ES 202 706-1 (2022) Environmental Engineering (EE); Metrics and measurement method for energy efficiency of wireless access network equipment; Part 1: Power consumption – static measurement method. ETSI Standard. https://www.etsi.org/deliver/etsi_es/202700_202799/20270601/01.07.01_60/es_20270601v010701p.pdf. Accessed 15 October 2024

EU 2012/19/EU (2012) Directive of the European Parliament and of the Council of 4 July 2012 on waste electrical and electronic equipment (WEEE). EUR-Lex. http://data.europa.eu/eli/dir/2012/19/oj. Accessed 15 October 2024

EU 2021/2279 (2021) Commission recommendation of 15 December 2021 on the use of the Environmental Footprint methods to measure and communicate the life cycle environmental performance of products and organisations. EUR-Lex. http://data.europa.eu/eli/reco/2021/2279/oj. Accessed 15 October 2024

Faist Emmenegger M, Frischknecht R, Stutz M, Guggisberg M, Witschi R, Otto T (2006) Life cycle assessment of the mobile communication system UMTS: Towards eco-efficient systems. Int J Life Cycle Ass 11:265-276. https://doi.org/10.1065/lca2004.12.193

Ficher M, Bauer T, Ligozat AL (2024) A comprehensive review of the end-of-life modeling in LCAs of digital equipment. Int J Life Cycle Ass. https://doi.org/10.1007/s11367-024-02367-x

Funtowicz SO, Ravertz JR (1990) Uncertainty and quality in science for policy. Springer, Netherlands. https://doi.org/10.1007/978-94-009-0621-1

Golard L, Louveaux J, Bol D (2023) Evaluation and projection of 4G and 5G RAN energy footprints: The case of Belgium for 2020-2025. Ann Telecommun 78(5):313-327. https://doi.org/10.1007/s12243-022-00932-9

Golard L, Agram Y, Rottenberg F, Quitin F, Bol D, Louveaux J (2024) A parametric power model of multi-band sub-6 GHz cellular base stations using on-site measurements. IEEE 35th Annual International Symposium on Personal, Indoor and Mobile Radio Communications (PIMRC). http://hdl.handle.net/2078.1/289070

Guérid J, Doré J B, Reverdy J, Reig B, Clemente A, Di Cioccio L (2022) Toward eco-design of a 5G mmWave transmitarray antenna based on life cycle assessment. Joint European Conference on Networks and Communications & 6G Summit (EuCNC/6G Summit). https://doi.org/10.1109/EuCNC/6GSummit54941.2022.9815659

Hauschild MZ, Rosenbaum RK, Olsen SI (2018) Life cycle assessment: Theory and practice. Springer, Switzerland. https://doi.org/10.1007/978-3-319-56475-3

Hauschild MZ, Kara S, Røpke I (2020) Absolute sustainability: Challenges to life cycle engineering. CIRP Ann-Manuf Techn 69(2):533-553. https://doi.org/10.1016/j.cirp.2020.05.004

Heijungs R (2024) Probability, statistics and life cycle assessment: Guidance for dealing with uncertainty and sensitivity. Springer, Switzerland. https://doi.org/10.1007/978-3-031-49317-1

Hess JC (2024) Chip production's ecological footprint: Mapping climate and environmental impact. Interface. https://www.interface-eu.org/publications/chip-productions-ecological-footprint. Accessed 15 October 2024

Hjalsted AW, Laurent A, Andersen MM, Olsen KH, Ryberg M, Hauschild MZ (2021) Sharing the safe operating space: Exploring ethical allocation principles to operationalize the planetary boundaries and assess absolute sustainability at individual and industrial sector levels. J Ind Ecol 25(1):6-19. https://doi.org/10.1111/jiec.13050

Humar I, Ge X, Xiang L, Jo M, Chen M, Zhang J (2011) Rethinking energy efficiency models of cellular networks with embodied energy. IEEE Network 25(2):40-49. https://doi.org/10.1109/MNET.2011.5730527

Hunter IC, Billonet L, Jarry B, Guillon P (2022) Microwave filters-applications and technology. IEEE T Microw Theory 50(3):794-805. https://doi.org/10.1109/22.989963

ISO 14040 (2006) Environmental management – Life cycle assessment – Principles and framework. ISO Standard. https://www.iso.org/standard/37456.html. Accesses 15 October 2024

ITF (2022) Mode choice in freight transport. OECD Research Reports. https://doi.org/10.1787/3e69ebc4-en

ITU-T L.1410 (2014) Methodology for the assessment of the environmental impact of information and communication technology goods, networks and services. ITU Recommendation. https://www.itu.int/rec/T-REC-L.1410-201412-I. Accessed 15 October 2024

ITU-T L.1470 (2020) Greenhouse gas emissions trajectories for the information and communication technology sector compatible with the UNFCCC Paris Agreement. ITU Recommendation. https://www.itu.int/rec/T-REC-L.1470-202001-I. Accessed 15 October 2024

Jung BH, Leem H, Sung DK (2014) Modeling of power consumption for macro-, micro-, and RRH-based base station architectures. IEEE 79th Vehicular Technology Conference (VTC Spring). https://doi.org/10.1109/VTCSpring.2014.7022990

Khan F (2009) LTE for 4G mobile broadband – Air interface technologies and performance. Cambridge University Press, United Kingdom. https://doi.org/10.1017/CBO9780511810336

Kallio S, Okrasinski T, Salemink A, Tanskanen P (2021) From Abacus and Sundial to 5G. 12th International Symposium on Environmentally Concise Design and Inverse Manufacturing (EcoDesign)

Kiemel S, Rietdorf C, Schutzbach M, Miehe R (2022) How to simplify life cycle assessment for industrial applications – A comprehensive review. Sustainability 14(23):15704. https://doi.org/10.3390/su142315704

Krishnan N, Williams ED, Boyd SB (2008) Case studies in energy use to realize ultra-high purities in semiconductor manufacturing. IEEE International Symposium on Electronics and the Environment. https://doi.org/10.1109/ISEE.2008.4562913

Lai X, Wang Y, Chen Q, Gu H, Zheng Y (2024) Carbon emission assessment of lithium iron phosphate batteries throughout lifecycle under communication base station in China. Sci Total Environ 949:175123. https://doi.org/10.1016/j.scitotenv.2024.175123

Larmo A, Lindström M, Meyer M, Pelletier G, Torsner J, Wiemann H (2009) The LTE link-layer design. IEEE Commun Mag 47(4):52-59. https://doi.org/10.1109/MCOM.2009.4907407

Limpert E, Stahel W A, Abbt M (2001) Log-normal distributions across the sciences: Keys and clues: on the charms of statistics, and how mechanical models resembling gambling machines offer a link to a handy way to characterize log-normal distributions, which can provide deeper insight into variability and probability – Normal or log-normal: That is the question. Bioscience 51(5):341-352. https://doi.org/10.1641/0006-3568(2001)051[0341:LNDATS]2.0.CO;2

Lorincz J, Matijevic T (2014) Energy-efficiency analyses of heterogeneous macro and micro base station sites. Comput Electr Eng 40(2):330-349. https://doi.org/10.1016/j.compeleceng.2013.10.013

Lundén D, Malmodin J, Bergmark P, Lövehagen N (2022) Electricity consumption and operational carbon emissions of European telecom network operators. Sustainability 14(5):2637. https://doi.org/10.3390/su14052637

Madon M (2021) Developing a parameterized embodied emissions calculator for telecommunication networks equipment (PEEC). Dissertation, KTH School of Electrical Engineering and Computer Science

Malmodin J, Oliv L, Bergmark P (2001) Life cycle assessment of third generation (3G) wireless telecommunication systems at Ericsson. Second International Symposium on Environmentally Conscious Design and Inverse Manufacturing. https://doi.org/10.1109/ECODIM.2001.992375

Malmodin J, Lundén D, Moberg Å, Andersson G, Nilsson M (2014) Life cycle assessment of ICT: Carbon footprint and operational electricity use from the operator, national, and subscriber perspective in Sweden. J Ind Ecol 18(6):829-845. https://doi.org/10.1111/jiec.12145

Malmodin J, Lundén D (2018) The energy and carbon footprint of the global ICT and E&M sectors 2010-2015. Sustainability 10(9):3027. https://doi.org/10.3390/su10093027

Malmodin J, Lövehagen N, Bergmark P, Lundén D (2024) ICT sector electricity consumption and greenhouse gas emissions-2020 outcome. Telecommun Policy 48(3):102701 https://doi.org/10.1016/j.telpol.2023.102701

May GJ (2006) Standby battery requirements for telecommunications power. J Power Sources 158(2):1117-1123. https://doi.org/10.1016/j.jpowsour.2006.02.083

Richardson K, Steffen W, Lucht W, Bendtsen J, Cornell SE, Donges JF et al. (2023) Earth beyond six of nine planetary boundaries. Sci Adv 9(37):2458. https://doi.org/10.1126/sciadv.adh2458

Ruiz D, San Miguel G, Rojo J, Teriús-Padrón JG, Gaeta E, Arredondo MT et al. (2022) Life cycle inventory and carbon footprint assessment of wireless ICT networks for six demographic areas. Resour Conserv Recycl 176:105951. https://doi.org/10.1016/j.resconrec.2021.105951

Santarius T, Bieser JC, Frick V, Höjer M, Gossen M, Hilty LM et al. (2022) Digital sufficiency: conceptual Considerations for ICTs on a finite planet. Ann Telecommun 78(5):277-295. https://doi.org/10.1007/s12243-022-00914-x

Scarlat N, Prussi M, Padella M (2022) Quantification of the carbon intensity of electricity produced and used in Europe. Appl Energ 305:117901. https://doi.org/10.1016/j.apenergy.2021.117901

Scharnhorst W, Althaus HJ, Classen M, Jolliet O, Hilty LM (2005) The end of life treatment of second generation mobile phone networks: Strategies to reduce the environmental impact. Environ Impact Asses 25(5):540-566. https://doi.org/10.1016/j.eiar.2005.04.005

Scharnhorst W, Hilty LM, Jolliet O (2006a) Life cycle assessment of second generation (2G) and third generation (3G) mobile phone networks. Environ Int 32(5):656-675. https://doi.org/10.1016/j.envint.2006.03.001

Scharnhorst W, Althaus HJ, Hilty L, Jolliet O (2006b) Environmental assessment of end-of-life treatment options for a GSM 900 antenna rack. Int J Life Cycle Ass 11:425-436. https://doi.org/10.1065/lca2005.08.216

Scharnhorst W (2008) Life cycle assessment in the telecommunication industry: A review. Int J Life Cycle Ass 13:75-86. https://doi.org/10.1065/lca2006.11.285

Stobbe L, Richter N, Quaeck M, Knüfermann K, Druschke J, Fahland M et al. (2023) Umweltbezogene technikfolgenabschätzung mobilfunk in Deutschland – Projekt: UTAMO. Unweltbundesamt. https://www.umweltbundesamt.de/sites/default/files/medien/479/publikationen/texte_26-2023_umweltbezogene_technikfolgenabschaetzung_mobilfunk_in_deutschland.pdf. Accessed 15 October 2024

Tahseen HU, Mescia L, Catarinucci L (2023) A survey of five generations of MIMO multiband base station antennas. Radio Sci 58(7):e2023RS007725. https://doi.org/10.1029/2023RS007725

Tombaz S, Vastberg A, Zander J (2011) Energy-and cost-efficient ultra-high-capacity wireless access. IEEE Wirel Commun 18(5):18-24. https://doi.org/10.1109/MWC.2011.6056688

Wang W, Liu D, Zhang Y, Gong C (2017) Energy estimation and optimization platform for 4G and the future base station system early-stage design. China Commun 14(4):47-64. https://doi.org/10.1109/CC.2017.7927576

Wernet G, Bauer C, Steubing B, Reinhard J, Moreno-Ruiz E, Weidema B (2016) The ecoinvent database version 3 (part I): Overview and methodology. Int J Life Cycle Ass 21:1218-1230. https://doi.org/10.1007/s11367-016-1087-8

Yeung HWC (2022) Interconnected worlds: Global electronics and production networks in East Asia. Stanford University Press, California